

## P(2-VP) supported Ru(II) material as catalyst for H<sub>2</sub> production from the methanolysis of NaBH<sub>4</sub>

Melek Tercan, Elif Karacan Yeldir, Osman Dayan & Ayhan Oral

To cite this article: Melek Tercan, Elif Karacan Yeldir, Osman Dayan & Ayhan Oral (2020): P(2-VP) supported Ru(II) material as catalyst for H<sub>2</sub> production from the methanolysis of NaBH<sub>4</sub>, Inorganic and Nano-Metal Chemistry, DOI: [10.1080/24701556.2020.1749077](https://doi.org/10.1080/24701556.2020.1749077)

To link to this article: <https://doi.org/10.1080/24701556.2020.1749077>



Published online: 06 May 2020.



Submit your article to this journal [↗](#)



Article views: 22



View related articles [↗](#)



View Crossmark data [↗](#)



## P(2-VP) supported Ru(II) material as catalyst for H<sub>2</sub> production from the methanolysis of NaBH<sub>4</sub>

Melek Tercan, Elif Karacan Yeldir, Osman Dayan , and Ayhan Oral

Department of Chemistry, Faculty of Arts and Science, Canakkale Onsekiz Mart University, Canakkale, Turkey

### ABSTRACT

Existing energy resources are not sufficient to meet the energy needs of the increasing world population so the need for clean and renewable energy systems is increasing day after day. Hydrogen is a good alternative energy source because of its clean by-products and high energy capacity. Studies on hydrogen storage systems that provide instant hydrogen production in the literature are of great interest. In this study, poly-2-vinylpyridine (p(2-VP)) polymer was prepared by photopolymerization method and reacted with 2,6-bis(2-benzimidazolyl)pyridine ligand containing Ru(II) complex to give p(2-VP) supported Ru(II) material. The synthesized Ru(II) complex was characterized by FT-IR, UV-Vis and <sup>1</sup>H-NMR spectroscopic techniques. Also the p(2-VP) polymer was characterized by FT-IR spectroscopy. The obtained p(2-VP) supported Ru(II) material was used as catalyst in hydrogen generation from NaBH<sub>4</sub> methanolysis reaction and the reaction kinetic was investigated.

### ARTICLE HISTORY

Received 24 January 2020  
Accepted 10 March 2020

### KEYWORDS

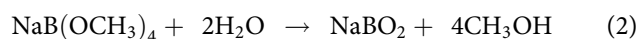
Hydrogen energy;  
ruthenium; benzimidazole  
type ligand; p(2-VP)  
polymer; methanolysis

## Introduction

The depletion and inadequacy of universal energy resources led researchers to develop new energy systems.<sup>[1]</sup> Considering the limitation of fossil fuels and the atmospheric pollution caused by the emission of greenhouse gases, the use of renewable energy sources is becoming more and more important. Hydrogen is a good alternative for renewable energy by its source-independent character and high potential to be a clean energy.<sup>[2-5]</sup> Also its high energy content compared to petroleum (44 MJ kg<sup>-1</sup> for petroleum and 120 MJ kg<sup>-1</sup> for hydrogen) makes it important for industry.<sup>[6]</sup> However, the efficient storage of hydrogen, safe and economic distribution systems are still an issue.<sup>[7,8]</sup> The US Department of Energy (DOE) has set the system capacity in vehicles as 62 kg H<sub>2</sub>/m<sup>3</sup> at specified temperature and pressure.<sup>[9]</sup> Hydrogen can be stored in liquefied form in high pressured tanks filled with sorbent materials. However, due to the difficulties in cryogenic hydrogen storage systems, the development of solid H<sub>2</sub> storage systems is essential.<sup>[9,10]</sup> There are some features sought in systems to be used in hydrogen storage:

- Hydrogen storage capacities of the materials
- High gravimetric H<sub>2</sub> capacities
- Safety
- Low-cost
- Systems in which reversible dehydrogenation is thermodynamically favorable. The efficiency of a storage system is depend on recyclability.<sup>[10,11]</sup>

Sorbents (C materials, graphene, zeolite, activated C, metal-organic frameworks, nano structured and nano-porous materials), metal hydrides (NaBH<sub>4</sub>, LiBH<sub>4</sub>), chemical hydrides and B-N compounds (ammonia borane (H<sub>3</sub>N.BH<sub>3</sub>), borazine, polyborazylene) are used in dehydrogenation reactions commonly.<sup>[6,12,13]</sup> Recently, ammonia boranes are the most popular storage systems due to their high gravimetric hydrogen capacities, low molar masses and rechargeabilities.<sup>[14-23]</sup> But practical H<sub>2</sub> formation, suitable reaction conditions with many different methods and different catalysts makes metal hydrides still remain attractive.<sup>[11]</sup> Especially sodium borahydride (NaBH<sub>4</sub>) is widely studied in the literature because of its high hydrogen content (10.9% by mass), generation of four moles of hydrogen per mol of NaBH<sub>4</sub>, workability at mild reaction conditions and its relatively low cost.<sup>[24-26]</sup> At room temperature self-hydrolysis of NaBH<sub>4</sub> occurs in aqueous media but the reaction is very slow. Alternative solvents have been tried for this catalytic process, but the fastest reaction kinetics have been observed with methanol at low temperatures and even in the absence of catalyst (Eq (1)).<sup>[26,27]</sup> Also the byproduct of methanolysis, sodium tetramethoxyborate (NaB(OCH<sub>3</sub>)<sub>4</sub>) can be regenerated to methanol through hydrolysis (Eq (2)).



Besides the advantages of NaBH<sub>4</sub> as nontoxic and non-flammable, hydrogen release via NaBH<sub>4</sub> is a controllable hydrolysis reaction, because the reaction starts with

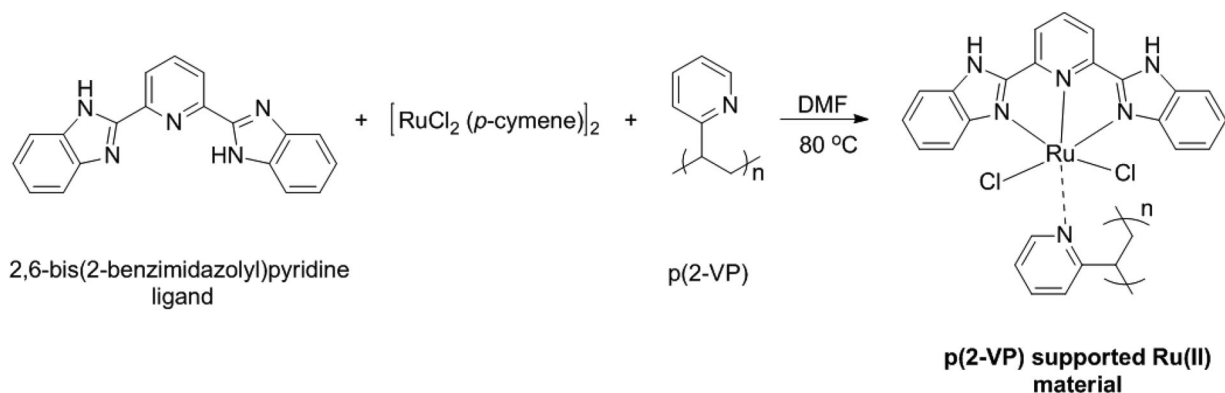


**Figure 1.** Schematical show of the preparation of p(2-VP) supported Ru(II) material.

catalyst.<sup>[28–30]</sup> Various catalyst systems, generally metal catalysts, were used to produce hydrogen from  $\text{NaBH}_4$  hydrolysis and metanolysis reactions.<sup>[31–37]</sup> Hydrogen obtained in hydrogen storage systems should be transported by surface diffusion. That is, hydrogen is obtained on the first surface and adsorbs on another surface. The first surface is usually a metal center, the second surface is a support material in which the metal is doped.<sup>[9]</sup> Therefore, the choice of the catalyst and the support material to immobilize the catalyst are important. The use of active and stable transition metals such as Ru, Pt in catalytic applications requires effective reduction of the metal. By using a low amount of metal by weight, more surface area per unit weight is obtained and metal aggregation is prevented. For this purpose, various support materials are used as alumina, silica, MOFs etc. However, during the contact of metal hydride with water, formation of B-O-based compounds and borates besides hydrogen causes an increase in the alkalinity and catalytic efficiency decreases as a result.<sup>[7]</sup> So, the chemical stability of the support material is as important as the surface area, porosity etc. and a polymer supported catalyst system can be a good option for catalysis.<sup>[37–40]</sup>

In this study, polypyridine type ligand bearing ruthenium(II) complex was chosen as catalysts and poly-2-vinylpyridine (p(2-VP)) polymer as a support material. 2-Vinylpyridine (2-VP) as a polymer template was polymerized by photopolymerization method, characterized by FT-IR spectroscopy. The p-(2-VP) polymer and Ru(II) complex were reacted in a certain ratio to obtain Ru metal-containing polymeric material and the metal content of the material was determined by SEM-EDX analysis. The obtained p(2-VP) supported Ru(II) material was used as catalyst in hydrogen generation from  $\text{NaBH}_4$  metanolysis reaction (Figure 1).

## Experimental

### Materials

#### Materials and apparatus

1,2-phenylenediamine (Alfa Aesar) and 2,6-pyridinedicarboxylic acid (Acros Organics) that used in the synthesis of 2,6-bis(2-benzimidazolyl)pyridine ligand were obtained commercially.  $\text{RuCl}_3 \cdot 3\text{H}_2\text{O}$  used in the preparation of

bis(dichloro(p-cymene)ruthenium (II)) dimer used in the complexation reaction was taken from Alfa Aesar. The benzoin used as initiator in the preparation of p(2-VP) polymer and the 2-VP used as monomer were obtained from Sigma Aldrich and Alfa Aesar. Tetrahydrofuran (THF), N,N-dimethylformamide (DMF), ortho-phosphoric acid that used as reaction solvents, and all solvents used in the separation-purification processes were obtained from Merck. Sodium tetrahydridoborate ( $\text{NaBH}_4$ ) and methanol that used in hydrogen generation reactions were purchased from Merck. Infrared spectra of the ligand, polymer and the material were recorded with Perkin Elmer Spectrum One FT-IR system using ATR sampling accessory. The  $^1\text{H-NMR}$  spectrum of the 2,6-bis(2-benzimidazolyl)pyridine ligand was recorded with a JEOL NMR – 400 MHz. The SEM image of the prepared polymer supported Ru(II) material was taken with JEOL – SEM – 7100 – EDX, while the XRD pattern of the material was recorded by Panalytical Empyrean X-Ray diffractometer.

#### Synthesis of 2,6-bis(2-benzimidazolyl)pyridine

The tri-dentate NN'N'' ligand, 2,6-bis(2-benzimidazolyl)pyridine, was synthesized according to the related literature.<sup>[41,42]</sup> Pyridine-2,6-dicarboxylic acid (20 mmol, 3.35 g) was added to 1,2-phenylenediamine (44 mmol, 4.7 g) in phosphoric acid (40 mL). The reaction mixture was stirred during 4 hours under Ar atmosphere. The obtained blue colored melt was poured into ice and after reaching room temperature, filtered off. Then sodium carbonate (10%, 100 mL) solution was added to the filtrate. The obtained pink-purple melt was washed with methanol numbers of times. And the solid was crystallized from MeOH. The orange crystals were purified by adding activated carbon. After recrystallization from methanol white-beige crystals were obtained.

FT-IR (ATR/ $\text{cm}^{-1}$ ): 3181, 3064, 1681, 1603, 1576, 1490, 1457, 1434, 1409, 1386, 1317, 1277, 1230, 1144, 1112, 1012, 958, 926, 845, 815, 738, 729, 693.  $^1\text{H-NMR}$  (400 MHz, DMSO- $d_6$ )  $\delta$  ppm 8.34 (d,  $J=7.37$  Hz, 2H), 8.17 (t,  $J=8.14$  Hz, 1H), 7.77 (d,  $J=7.74$  Hz, 2H), 7.74 (d,  $J=8.34$  Hz, 2H), 7.35 (t,  $J=7.69$  Hz, 2H), 7.28 (t,  $J=7.46$  Hz, 2H).

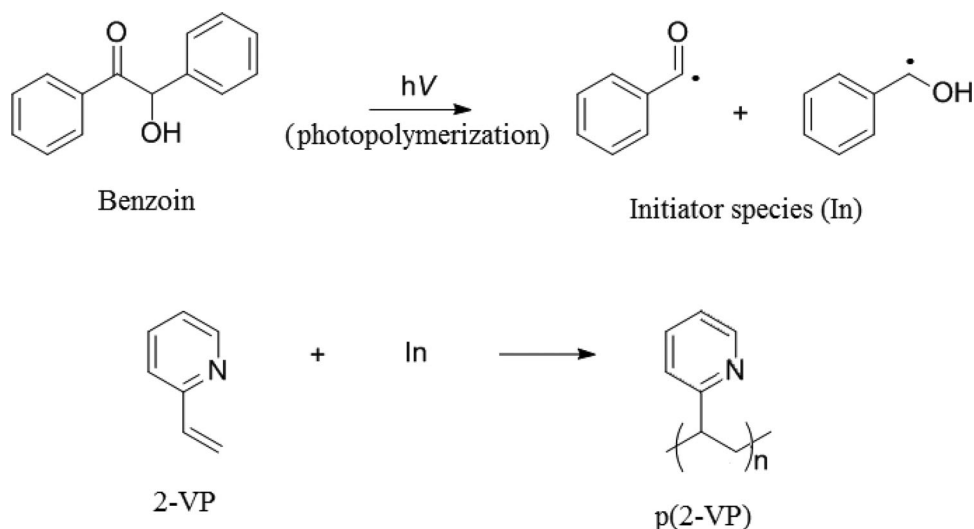


**Figure 2.** The preparation of p(2-VP) by photopolymerization.

### Synthesis of poly(2-vinylpyridine), p(2-VP)

Benzoin was used as a type I photoinitiator and tetrahydrofuran (THF) was used as solvent in the polymerization of 2-VP. Initiator an amount of 1% of by mass of the monomer was placed into quartz tube and degassed with nitrogen. Then, THF and the monomer, 2-VP, were added into tube under N<sub>2</sub> atmosphere. Photopolymerization occurred at 310 nm for benzoin. The contents of tube was dissolved in methanol after specified time (1.5, 3, 6, 9, 12 and 24 h). The polymer was precipitated with diethyl ether, then filtered and washed with diethyl ether for three times.

### Synthesis of p(2-VP) supported Ru(II) material

The tridentate 2,6-bis(2-benzimidazolyl)pyridine ligand (100 mg, 0.321 mmol) was dissolved in DMF (10 mL) and dichloro(p-cymene)ruthenium (II) dimer (98 mg, 0.161 mmol) was added. The reaction mixture was stirred at 50 °C until the color turned brown-cherry. Then p(2-VP) (337 mg, 3.21 mmol) was added to the media and stirred at 80 °C over night. The reaction solvent was removed, the residue was washed with diethyl ether and allowed to dry. p(2-VP) supported Ru(II) material was obtained as brown solid.

FT-IR (ATR/cm<sup>-1</sup>): 3388, 3056, 3005, 2927, 2851, 1709, 1623, 1589, 1568, 1473, 1433, 1359, 1318, 1222, 1148, 1085, 1049, 994, 914, 857, 748.

### The catalytic tests

The H<sub>2</sub> generation reactions via NaBH<sub>4</sub> hydrolysis were carried out by water displacement method. 20 mL of deionized water (or methanol) was placed into a 50 mL two-necked flask, NaBH<sub>4</sub> (125 mM) was added and H<sub>2</sub> generation was investigated at 1000 rpm mixing rate at 25 °C. H<sub>2</sub> generation from the self-hydrolysis/methanolysis of NaBH<sub>4</sub> were tested first without catalyst. Then, the catalytic performance of p(2-VP) supported Ru(II) material as catalyst was determined. H<sub>2</sub> generation was investigated in the presence of different amounts (10, 25, 50, 100 mg) of p(2-VP) supported

Ru(II) material catalysts. A series of methanolysis tests were carried out for various temperatures (0 °C, 15 °C, 25 °C, 35 °C, 45 °C) to examine the kinetics.

## Results and discussion

### Characterization of p(2-VP) and p(2-VP) supported Ru(II) material catalyst

P(2-VP) polymer was prepared by photopolymerization method (Figure 2). Then p(2-VP) supported Ru(II) material was prepared according to the procedure at 2.4. The morphology and the distribution of metal in the synthesized p(2-VP) supported Ru(II) material was examined by SEM coupled EDX, the images at different magnifications are given in Figure 3.

As shown in Figure 3, it is possible to say that the obtained p(2-VP) supported Ru(II) material is homogeneous. In addition, as a result of EDX measurements taken from different sections of the spectra, Ru composition is observed in the range of 0.4-0.5% and supports homogeneity. The overlapped XRD spectra of p(2-VP) polymer and the p(2-VP) supported Ru(II) material is given in Figure 4. With the extension of the p(2-VP) polymer chain, the amount of Ru per chain is reduced. Therefore, the Ru peak was suppressed and could not be observed in the XRD pattern. In addition, the peaks of the p(2-VP) polymer were sharper, while the p(2-VP) supported Ru(II) material peaks showed spreading and this indicates amorphous structure.

The overlapped FT-IR spectra of p(2-VP), tri-dentate ligand, (2,6-bis(2-benzimidazolyl)pyridine), and p(2-VP) supported Ru(II) material are given in Figure 5. When the FT-IR spectrum of p(2-VP) supported Ru(II) material was examined, aromatic C-H stretching peaks were observed at 3056 and 3005 cm<sup>-1</sup>. The peaks monitored at 2927 and 2851 cm<sup>-1</sup> are belong to aliphatic CH<sub>2</sub> and CH stretching peaks of p(2-VP) and prove that the material contains the p(2-VP) polymer. The C=N double bond stretching peak of (2,6-bis(2-benzimidazolyl)pyridine) ligand at 1681 cm<sup>-1</sup> was shifted to 1709 cm<sup>-1</sup> in the spectrum of Ru(II) material.

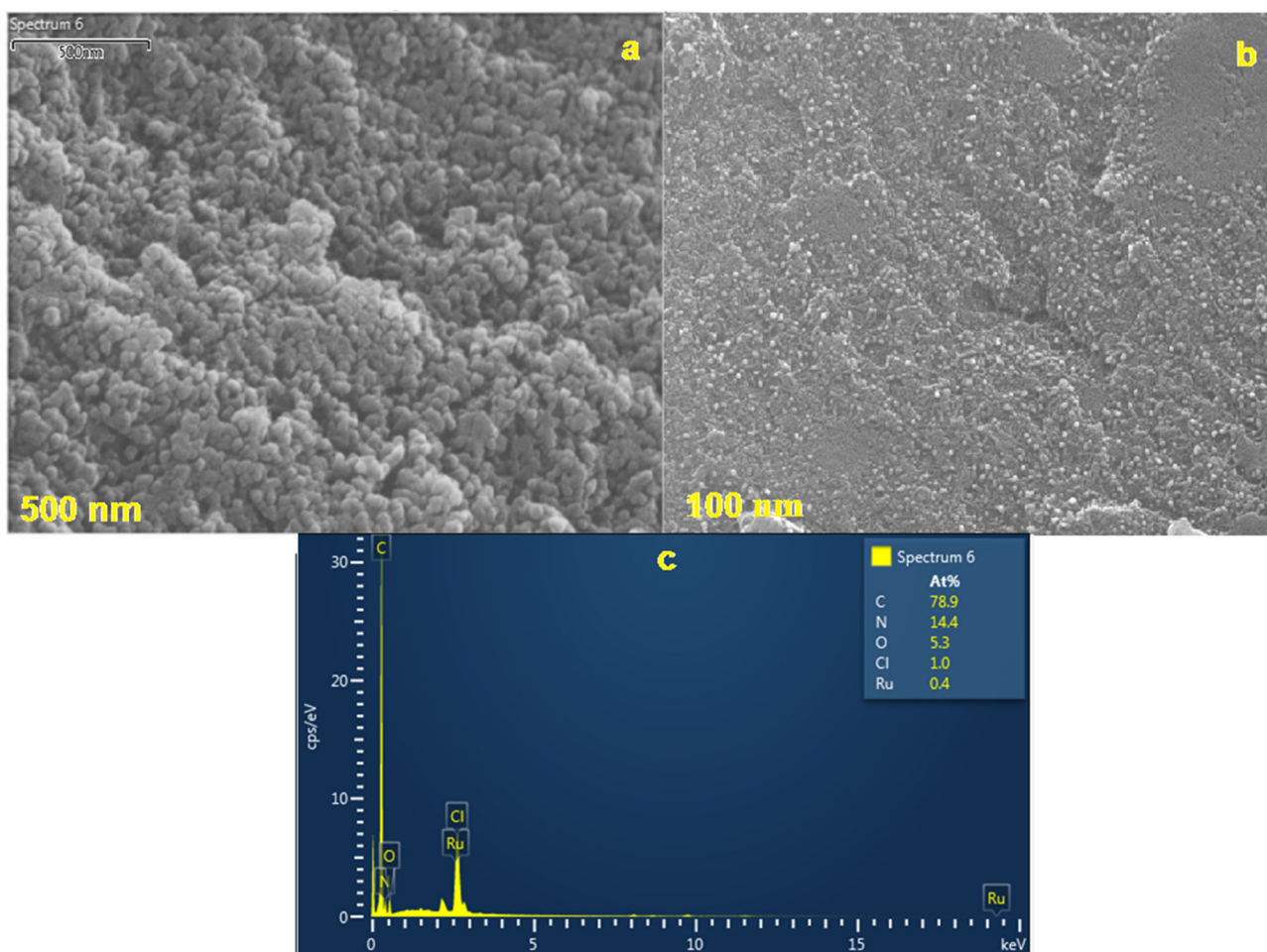


Figure 3. (a,b) SEM images of p(2-VP) supported Ru(II) material (c) EDX of p(2-VP) supported Ru(II) material.

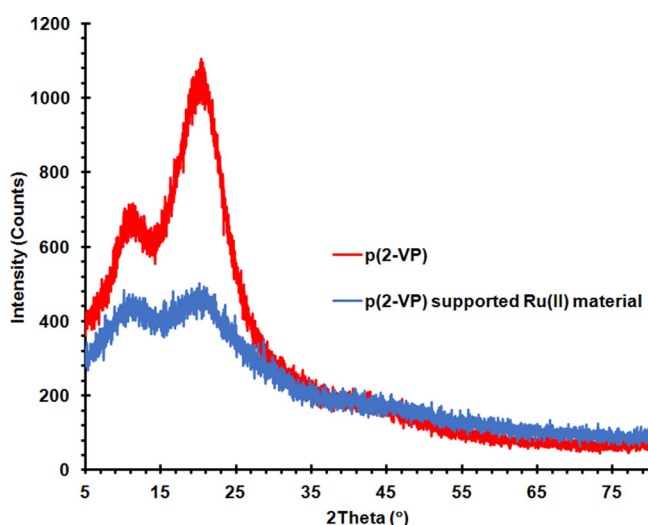


Figure 4. XRD patterns of p(2-VP) (red line) and p(2-VP) supported Ru(II) material (blue line).

Also, the aromatic C=C double bond stretching peaks were observed in the range of  $1589\text{--}1433\text{ cm}^{-1}$  and support the structure.

$^1\text{H-NMR}$  spectra of p(2-VP) and p(2-VP) supported Ru(II) material are very similar. As shown in Figure 6, the aromatic protons are observed around 6.00 – 8.50 ppm

region. On the other hand, the signals at 1.30–1.90 ppm are assigned to aliphatic protons. Also, the -H<sub>x,y</sub> protons of p(2-VP) supported Ru(II) material are monitored at 7.50 – 8.00 ppm region. The other hydrogen peaks belong to benzimidazole ring maybe overlapped with p(2-VP) aromatic hydrogens peaks.

Also, p(2-VP) and p(2-VP) supported Ru(II) complex were studied by thermogravimetric analysis from ambient temperature to 1000 °C in a nitrogen atmosphere (Figure 7). According to Figure 7, both compounds decompose in two steps between 50 and 1000 °C while p(2-VP) supported Ru(II) complex is more stable.

#### Catalytic performance of p(2-VP) supported Ru(II) material H<sub>2</sub> generation via NaBH<sub>4</sub> methanolysis

P(2-VP) supported Ru(II) material was used as catalyst in H<sub>2</sub> generation from NaBH<sub>4</sub>. For this purpose, hydrolysis and methanolysis reactions of NaBH<sub>4</sub> were compared in catalyst-free medium and it is observed that the methanolysis of NaBH<sub>4</sub> reaction is faster. The generated volume of H<sub>2</sub> by the hydrolysis reaction was 82 mL after 2 hours, while after 10 minutes by methanolysis the reaction was almost complete and about 165 mL of H<sub>2</sub> was collected. Therefore, methanolysis of NaBH<sub>4</sub> reactions were used in all catalytic

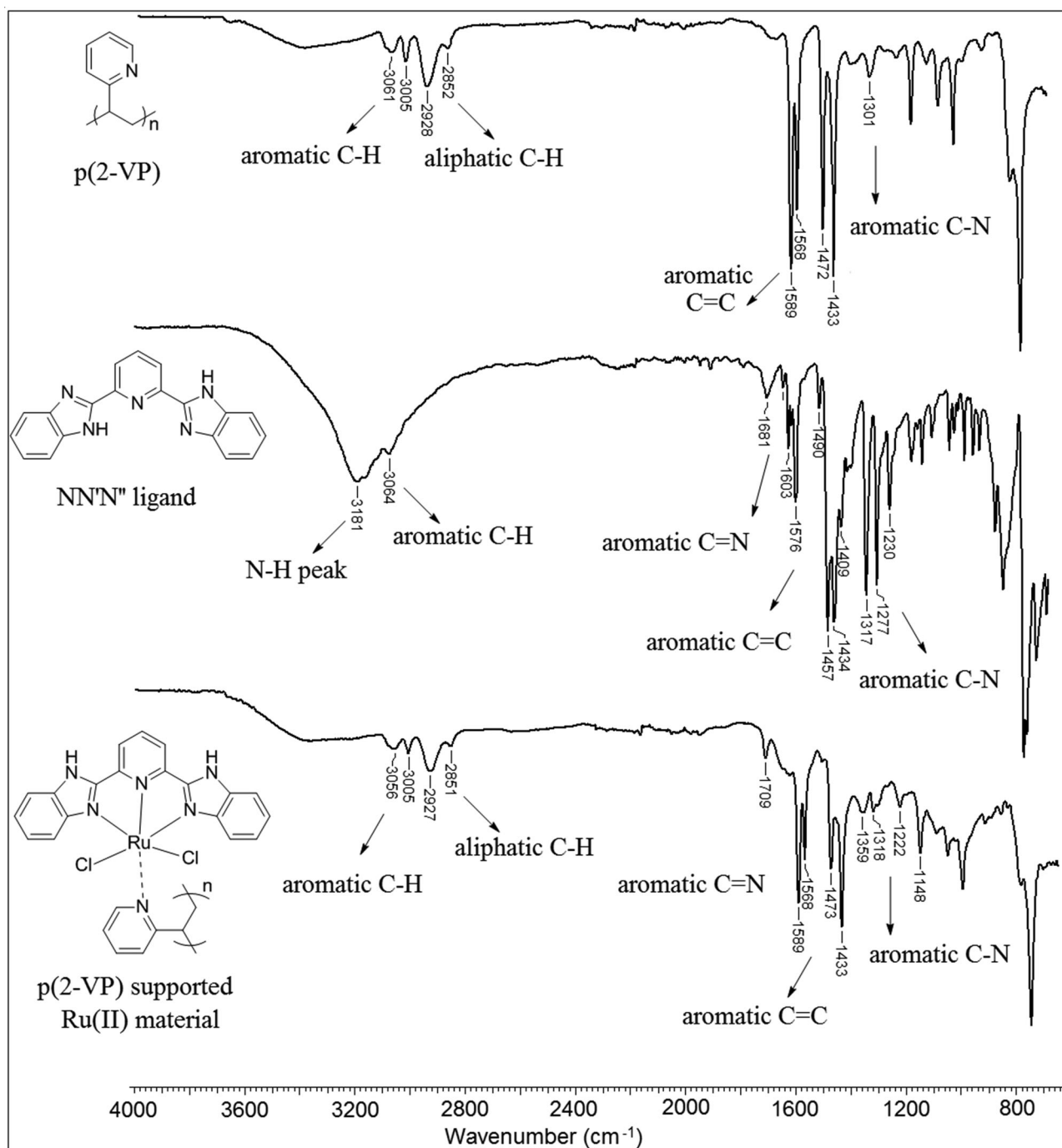


Figure 5. Overlapped FT-IR spectra of p(2-VP), NN'N'' ligand (2,6-bis(2-benzimidazolyl)pyridine) and p(2-VP) supported Ru(II) material.

studies to investigate the catalytic performance of the p(2-VP) supported Ru(II) material.

#### The effect of amount of catalyst on H<sub>2</sub> generation

In order to investigate the effectiveness of the prepared material in H<sub>2</sub> generation reactions via methanolysis of NaBH<sub>4</sub>, some parameters such as catalyst amount and temperature were changed in the catalytic experiments. The prepared p(2-VP) supported Ru(II) material has a very low metal content of about 0.4% (Figure 3), and supported catalysts with low metal content are important for catalyst

chemistry because of their environmental friendliness. To determine the effect of catalyst amount, p(2-VP) supported Ru(II) material weighing in the range of 10–100 mg were used as catalyst in methanolysis of NaBH<sub>4</sub> (125 mM, 20 mL) at room temperature (25 °C) with 1000 rpm mixing rate. All catalytic trials were performed in triplicate using 10, 25, 50 and 100 mg of catalyst, respectively. In the experiments, it was observed that all methanolysis reactions were completed in about 5 minutes, after this time no significant changes were observed and the generated H<sub>2</sub> volumes were almost constant until the end of 20 minutes. The average volume of hydrogen collected at the end of 5 min for the methanolysis

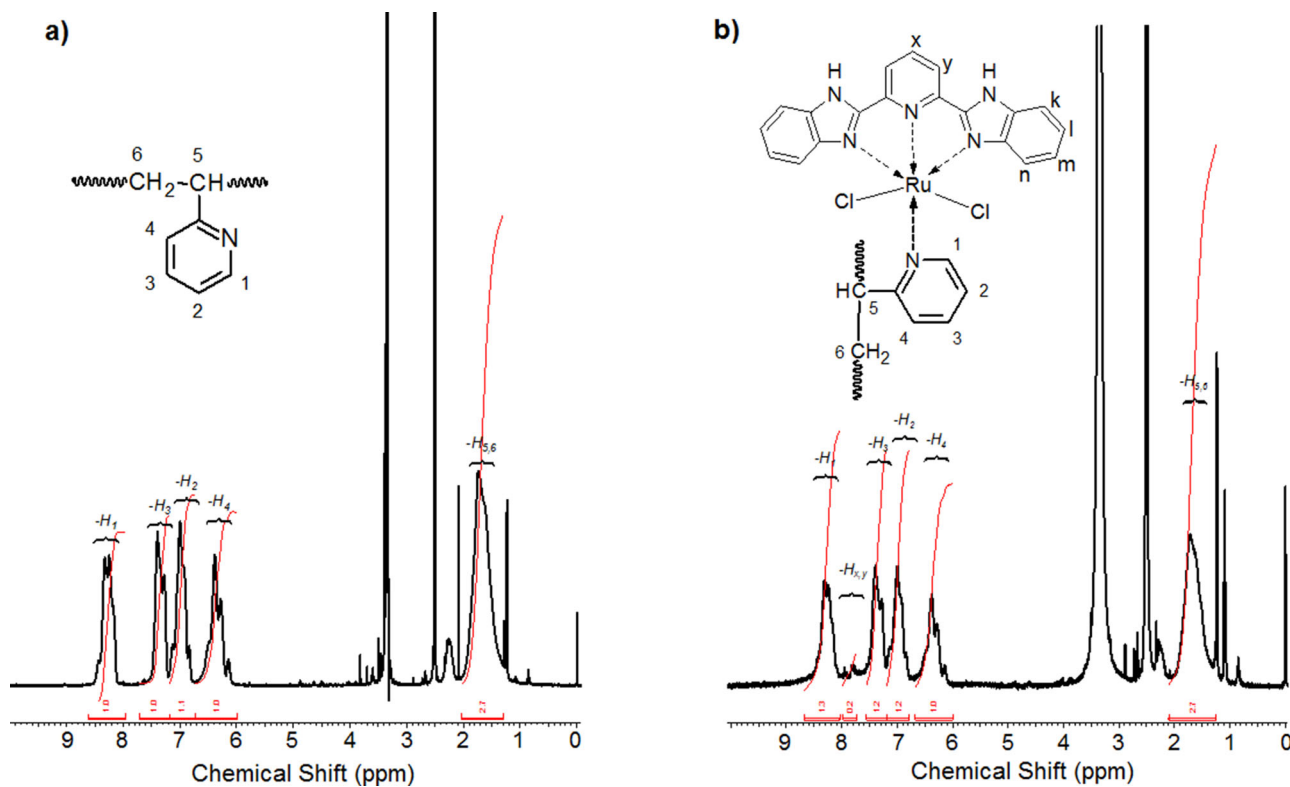


Figure 6.  $^1\text{H-NMR}$  spectra of p(2-VP) (a) and p(2-VP) supported Ru(II) material (b).

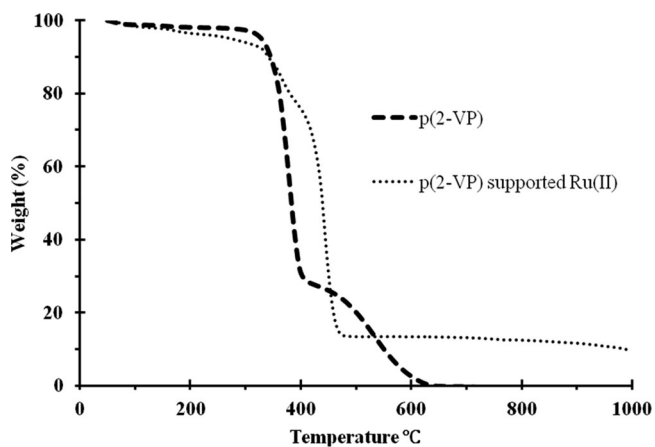


Figure 7. TG curves of p(2-VP) and p(2-VP) supported Ru(II) complex.

reaction that 10 mg of catalyst used was  $149 \pm 7$  mL, while  $148 \pm 5$  mL,  $167 \pm 0.4$  mL and  $170 \pm 6$  mL were observed for 25 mg, 50 mg and 100 mg, respectively (Figure 8a). An inverse proportion was observed between  $\text{H}_2$  generation rates (HGR) and the amount of catalyst used. The HGR values were calculated up to 5 min of the methanolysis reaction time as  $2980 \pm 71$ ,  $1192 \pm 11$ ,  $669 \pm 2$ ,  $339 \pm 13$  mL  $\text{min}^{-1}$   $g_{\text{catalyst}}^{-1}$  for 10, 25, 50 and 100 mg p(2-VP) supported Ru(II) material, respectively (Figure 8b). Since increasing the amount of catalyst above 50 mg practically results in an increase of only 2 mL of generated  $\text{H}_2$  volume (Figure 8c), this amount was not exceeded and the optimum amount of catalyst was determined as 50 mg. For this reason, the amount of catalyst was determined as 50 mg in the experiments in which the effect of temperature on the  $\text{H}_2$

generation reactions via methanolysis of  $\text{NaBH}_4$  was investigated (Table 1).

$$\text{H}_2\text{generation rate} = \frac{\text{(generated H}_2\text{ volume (mL))}}{\text{(time (min) } \times \text{ catalyst amount (g))}} \quad (3)$$

#### The effect of temperature on $\text{H}_2$ generation via methanolysis of $\text{NaBH}_4$

Catalytic experiments were carried out at varying temperatures (0 to  $45^\circ\text{C}$ ) using 50 mg catalyst under the same conditions (125 mM, 20 mL  $\text{NaBH}_4$ , 1000 rpm mixing rate) and activation energies were calculated for different temperatures. The methanolysis reaction of  $\text{NaBH}_4$  was completed at  $0^\circ\text{C}$  at the end of 20 min, and at 12, 8, 5 and 4 min at 15, 25, 35 and  $45^\circ\text{C}$ , respectively. As the temperature increased, both the reaction time was shortened and the collected hydrogen volume increased. The time-generated  $\text{H}_2$  volume graph by variation of the temperature is shown in Figure 9a. The generated  $\text{H}_2$  volume was observed as  $161 \pm 3$  mL,  $178 \pm 2$  mL,  $173 \pm 5$  mL,  $188 \pm 3$  mL and  $201 \pm 0.4$  mL for 0, 15, 25, 35 and  $45^\circ\text{C}$ , respectively. The activation energy of the reaction was calculated by using Arrhenius equation (Eq (4)) where,  $k$  is the rate constant,  $E_a$  is the activation energy,  $R$  is the ideal gas constant ( $8.314 \text{ j mol}^{-1} \text{ K}^{-1}$ ) and  $T$  is temperature (K). To calculate the reaction constant values ( $k$  values), the times required to collect the same amount of  $\text{H}_2$  at different temperature values are recorded. The reaction is the first order ( $R = k \cdot [A]^0$ ), so  $k$  values are equal to  $1/t$  ( $\text{s}^{-1}$ ) values. Thus, the  $k$  values of the methanolysis reactions of  $\text{NaBH}_4$  at different temperatures were determined, then the  $E_a$  of the reaction was calculated as  $53.9 \pm 2 \text{ kJ mol}^{-1}$  by

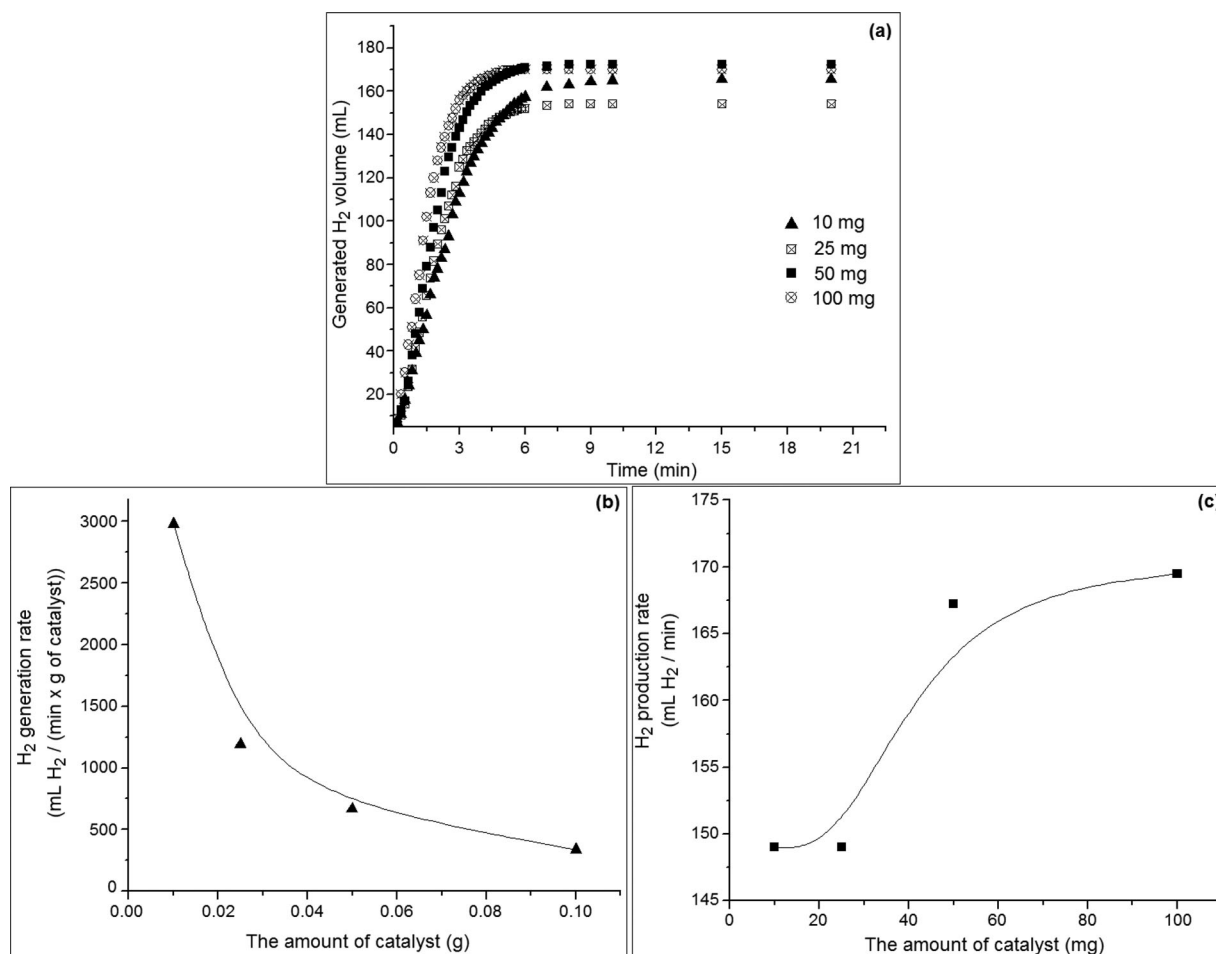


**Figure 8.** The effect of catalyst amount on methanolysis of NaBH<sub>4</sub> (a), the comparison of H<sub>2</sub> generation rates (b) and the comparison of reaction rates (c) (up to 5 min of reaction time).

**Table 1.** The effect of catalyst amount on generated H<sub>2</sub> volume and H<sub>2</sub> generation rate.

Catalyst amount (mg)	<sup>a</sup> Generated H <sub>2</sub> volume (mL)	<sup>b</sup> H <sub>2</sub> generation rate (mL min <sup>-1</sup> g <sub>catalyst</sub> <sup>-1</sup> )
10	149 ± 7	2980 ± 71
25	148 ± 5	1192 ± 11
50	167 ± 0.4	669 ± 2
100	170 ± 6	339 ± 13

<sup>a</sup>Average values of generated H<sub>2</sub> volume at the end of the 5 minutes in the methanolysis of NaBH<sub>4</sub> (125 mM, 20 mL) at room temperature (25 °C) with 1000 rpm mixing rate with different amount of catalyst (10, 25, 50 and 100 mg).

<sup>b</sup>H<sub>2</sub> generation rates were calculated by using Eq. (4).

plotting  $\ln k$  versus  $1/T$  graph (Figure 9b).  $E_a$  value for non-catalyst methanolysis reaction of NaBH<sub>4</sub> is reported as 62.99 kJ mol<sup>-1</sup> in the literature.<sup>[43]</sup> This result shows that the p(2-VP) supported Ru(II) catalyst material is comparable to expensive catalyst systems (Table 2).

$$\ln k = \ln A - (E_a/RT) \quad (4)$$

## Conclusions

In this study, p(2-VP) polymer was first synthesized by photopolymerization method. Then polymer supported Ru(II) material was prepared using the tri-dentate benzimidazole-type ligand 2,6-bis(2-benzimidazolyl)pyridine ligand and p(2-VP) polymer. The catalytic performance of supported

Ru(II) material, which has low metal content, was investigated in H<sub>2</sub> generation reactions via methanolysis of NaBH<sub>4</sub>. All catalytic measurements were made for the methanolysis reaction, since the amount of hydrogen generated was greater and the reaction was completed in a shorter time comparing with hydrolysis. Catalytic experiments were performed for different amounts of catalyst (10, 25, 50 and 100 mg) and best results were obtained as 167 ± 0.4 mL of generated hydrogen volume for 50 mg catalyst and 170 ± 7 mL for 100 mg catalyst at the end of 5 min for the methanolysis reaction. Subsequently, catalytic experiments were carried out at different temperature values (0, 15, 25, 35 and 45 °C) with 50 mg of catalyst under the same reaction conditions and the highest volume of generated hydrogen was observed as 201 ± 0.4 mL for 45 °C. The activation

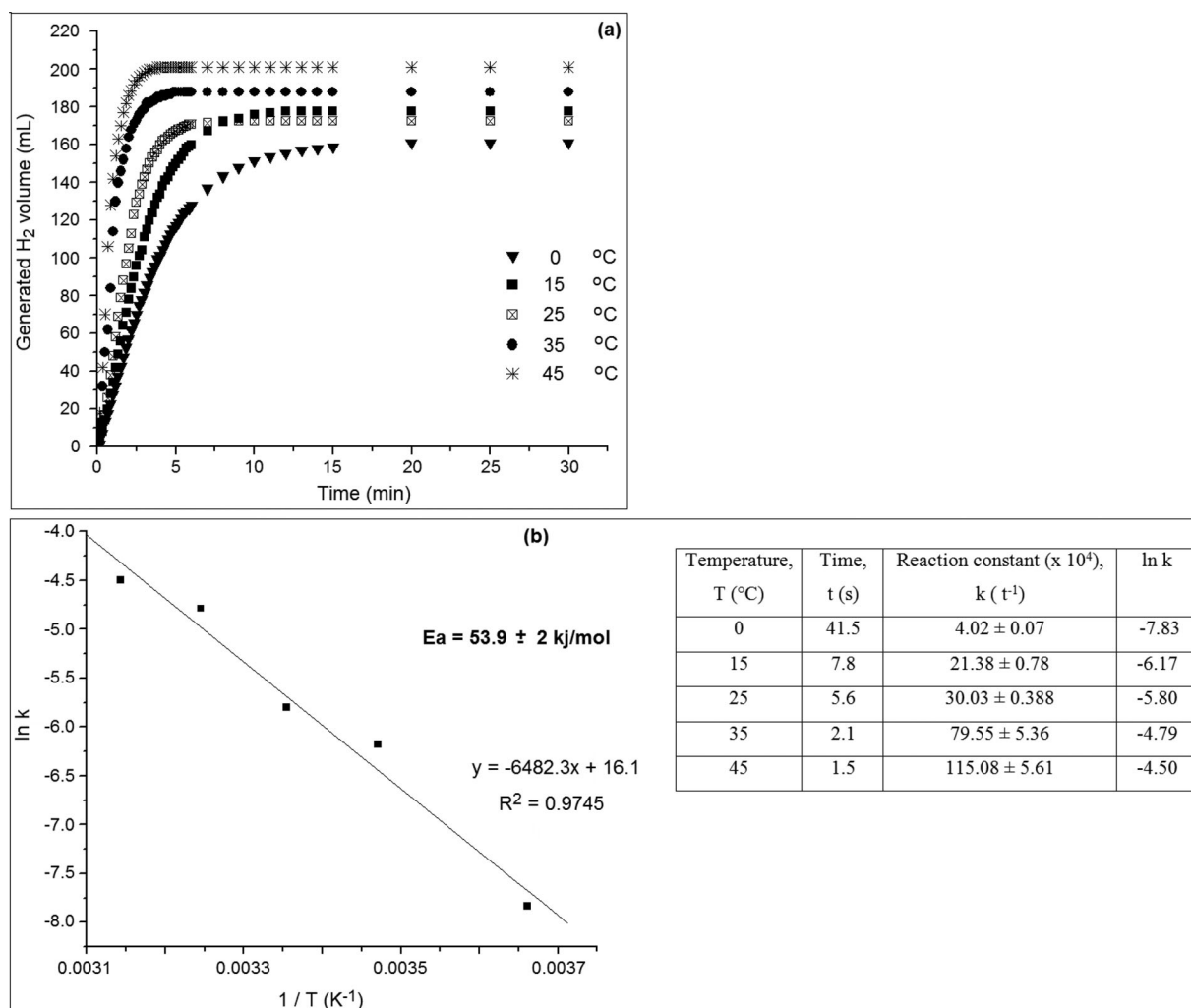


**Figure 9.** The effect of temperature on methanolysis of NaBH<sub>4</sub> (a) Arrhenius equation (lnk versus 1/T graph) (b).

**Table 2.** The completion times of the NaBH<sub>4</sub> methanolysis reaction and the maximum generated H<sub>2</sub> volumes at different temperature values.

Temperature (°C)	Completion time (min)	Generation H <sub>2</sub> volume (mL)
0	20.0	161 ± 3
15	12.0	178 ± 2
25	8.0	173 ± 5
35	4.8	188 ± 3
45	3.8	201 ± 0.4

Generated H<sub>2</sub> volumes at different temperature values are recorded for NaBH<sub>4</sub> (125 mM, 20 mL) with 1000 rpm mixing rate

energy ( $E_a$ ) of the reaction was calculated as  $53.9 \pm 2 \text{ kJ mol}^{-1}$ , which is lower than the  $E_a$  value of the catalyst-free methanolysis reaction of NaBH<sub>4</sub>. Although metal-free catalyst systems are preferred because they are cheaper and more environmentally friendly, metals and metal nanoparticle-based catalysts retain their superiority. And as a result of this study, it was observed that p(2-VP) polymer supported Ru(II) material, which can be an example for composite systems with low metal content, is suitable for hydrogenation studies.

## ORCID

Osman Dayan <http://orcid.org/0000-0002-0764-1965>

## References

- Demirci, S.; Sunol, A. K.; Sahiner, N. Catalytic Activity of Amine Functionalized Titanium Dioxide Nanoparticles in Methanolysis of Sodium Borohydride for Hydrogen Generation. *Appl Catal B: Environ.* **2020**, *261*, 118242. DOI: [10.1016/j.apcatb.2019.118242](https://doi.org/10.1016/j.apcatb.2019.118242).
- Turner, J.; Sverdrup, G.; Mann, M. K.; Maness, P. C.; Kroposki, B.; Ghirardi, M.; Evans, R. J.; Blake, D. Renewable Hydrogen Production. *Int. J. Energy Res.* **2008**, *32*, 379–407. DOI: [10.1002/er.1372](https://doi.org/10.1002/er.1372).
- Abdalla, A. M.; Hossain, S.; Nisfindy, O. B.; Azad, A. T.; Dawood, M.; Azad, A. K. Hydrogen Production, Storage, Transportation and Key Challenges with Applications: A Review. *A Rev. Energy Convers. Manag.* **2018**, *165*, 602–627. DOI: [10.1016/j.enconman.2018.03.088](https://doi.org/10.1016/j.enconman.2018.03.088).
- Zhou, L. Progress and Problems in Hydrogen Storage Methods. *Renew. Sustain. Energy Rev.* **2005**, *9*, 395–408. DOI: [10.1016/j.rser.2004.05.005](https://doi.org/10.1016/j.rser.2004.05.005).
- Bellotti, D.; Rivarolo, M.; Magistri, L.; Massardo, A. F. Thermo-Economic Comparison of Hydrogen and Hydro-Methane Produced from Hydroelectric Energy for Land Transportation. *J Hydrogen Energy* **2015**, *40*, 2433–2444. DOI: [10.1016/j.ijhydene.2014.12.066](https://doi.org/10.1016/j.ijhydene.2014.12.066).
- Hamilton, C. W.; Baker, T.; Staubitz, A.; Manners, I. B–N Compounds for Chemical Hydrogen Storage. *Chem. Soc. Rev.* **2009**, *38*, 279–293. DOI: [10.1039/B800312M](https://doi.org/10.1039/B800312M).
- Feng, C.; Wang, Y.; Gao, S.; Shang, N.; Wang, C. Hydrogen Generation at Ambient Conditions: AgPd Bimetal Supported on Metal–Organic Framework Derived Porous Carbon as an

- Efficient Synergistic Catalyst. *Catal. Commun.* **2016**, *78*, 17–21. DOI: [10.1016/j.catcom.2016.01.034](https://doi.org/10.1016/j.catcom.2016.01.034).
8. Park, J. H.; Shakkthivel, P.; Kim, H. J.; Han, M. K.; Jang, J. K.; Kim, Y. R.; Kim, H. S.; Shul, Y. G. Investigation of Metal Alloy Catalyst for Hydrogen Release from Sodium Borohydride for Polymer Electrolyte Membrane Fuel Cell Application. *Int. J. Hydrogen Energy* **2008**, *33*, 1845–1852. DOI: [10.1016/j.ijhydene.2008.01.003](https://doi.org/10.1016/j.ijhydene.2008.01.003).
  9. Wang, L.; Yang, R. T. New Sorbents for Hydrogen Storage by Hydrogen Spillover – a Review. *Energy Environ. Sci.* **2008**, *1*, 268–279. DOI: [10.1039/b807957a](https://doi.org/10.1039/b807957a).
  10. Orimo, S. I.; Nakamori, Y.; Eliseo, J. R.; Züttel, A.; Jensen, C. M. Complex Hydrides for Hydrogen Storage. *Chem. Rev.* **2007**, *107*, 4111–4132. DOI: [10.1021/cr0501846](https://doi.org/10.1021/cr0501846).
  11. Davis, B. L.; Dixon, D. A.; Garner, E. B.; Gordon, J. C.; Matus, M. H.; Scott, B.; Stephens, F. H. Efficient Regeneration of Partially Spent Ammonia Borane Fuel. *Angew. Chem. Int. Ed.* **2009**, *48*, 6812–6816. DOI: [10.1002/anie.200900680](https://doi.org/10.1002/anie.200900680).
  12. Nunes, H. X.; Ferreira, M. J. F.; Rangel, C. M.; Pinto, A. Hydrogen Generation and Storage by Aqueous Sodium Borohydride (NaBH<sub>4</sub>) Hydrolysis for Small Portable Fuel Cells (H<sub>2</sub>-PEMFC). *Int. J. Hydrogen Energy* **2016**, *41*, 15426–15432. DOI: [10.1016/j.ijhydene.2016.06.173](https://doi.org/10.1016/j.ijhydene.2016.06.173).
  13. Xueping, Z.; Xiangsheng, Y.; Xinyue, L.; Runnan, J.; Yongsheng, Z.; Zhihao, Z.; Xuzhao, H.; Yan, Z.; Gang, Z.; Yiqiong, P. Hydrogen Storage Performance of HPSB Hydrogen Storage Materials. *Chem. Phys. Lett.* **2019**, *734*, 136697. DOI: [10.1016/j.cplett.2019.136697](https://doi.org/10.1016/j.cplett.2019.136697).
  14. Bluhm, M. E.; Bradley, M. G.; Butterick, R.; Kusari, U.; Sneddon, L. G. Amineborane-Based Chemical Hydrogen Storage: Enhanced Ammonia Borane Dehydrogenation in Ionic Liquids. *J. Am. Chem. Soc.* **2006**, *128*, 7748–7749. DOI: [10.1021/ja062085v](https://doi.org/10.1021/ja062085v).
  15. Denney, M. C.; Pons, V.; Hebden, T. J.; Heinekey, D. M.; Goldberg, K. I. Efficient Catalysis of Ammonia Borane Dehydrogenation. *J. Am. Chem. Soc.* **2006**, *128*, 12048–12049. DOI: [10.1021/ja062419g](https://doi.org/10.1021/ja062419g).
  16. Keaton, R. J.; Blacquiere, J. M.; Baker, R. T. Base Metal Catalyzed Dehydrogenation of Ammonia-Borane for Chemical Hydrogen Storage. *J. Am. Chem. Soc.* **2007**, *129*, 1844–1845. DOI: [10.1021/ja066860i](https://doi.org/10.1021/ja066860i).
  17. Smythe, N. C.; Gordon, J. C. Ammonia Borane as a Hydrogen Carrier: Dehydrogenation and Regeneration. *Eur. J. Inorg. Chem.* **2010**, *2010*, 509–521. DOI: [10.1002/ejic.200900932](https://doi.org/10.1002/ejic.200900932).
  18. Stephens, F. H.; Pons, V.; Baker, R. T. Ammonia-Borane: The Hydrogen Source Par Excellence? *Dalton Trans.* **2007**, *1*, 2613–2626. DOI: [10.1039/B703053C](https://doi.org/10.1039/B703053C).
  19. Sutton, A. D.; Burrell, A. K.; Dixon, A. D.; Garner, E. B.; Gordon, J. C.; Nakagawa, T.; Ott, K. C.; Robinson, J. P.; Vasiliu, M. Regeneration of Ammonia Borane Spent Fuel by Direct Reaction with Hydrazine and Liquid Ammonia. *Science* **2011**, *331*, 1426–1429. DOI: [10.1126/science.1199003](https://doi.org/10.1126/science.1199003).
  20. Metin, Ö.; Mazumder, V.; ÖZkar, S.; Sun, S. ; Monodisperse Nickel Nanoparticles and Their Catalysis in Hydrolytic Dehydrogenation of Ammonia Borane. *J. Am. Chem. Soc.* **2010**, *132*, 1468–1469. DOI: [10.1021/ja909243z](https://doi.org/10.1021/ja909243z).
  21. Sun, D.; Mazumder, V.; Metin, O.; Sun, S. Catalytic Hydrolysis of Ammonia Borane via Cobalt Palladium Nanoparticles. *ACS Nano* **2011**, *5*, 6458–6464. DOI: [10.1021/nn2016666](https://doi.org/10.1021/nn2016666).
  22. Metin, O.; Kayhan, E.; Ozkar, S.; Schneider, J. J. Palladium Nanoparticles Supported on Chemically Derived Graphene: An Efficient and Reusable Catalyst for the Dehydrogenation of Ammonia Borane. *Int. J. Hydrogen Energy* **2012**, *37*, 816–8169.
  23. Can, H.; Metin, O. A Facile Synthesis of Nearly Monodisperse Ruthenium Nanoparticles and Their Catalysis in the Hydrolytic Dehydrogenation of Ammonia Borane for Chemical Hydrogen Storage. *Appl Cat B: Environ* **2012**, *125*, 304–310. DOI: [10.1016/j.apcatb.2012.05.048](https://doi.org/10.1016/j.apcatb.2012.05.048).
  24. Han, M. K.; Han, J. H.; An, K. J.; Jeon, D. S.; Gervasio, D.; Song, I. H.; Lee, Y. M.; Shul, Y. G. Study on a Reactor Design and Catalyst for Hydrogen Generation from Alkaline Solution of Sodium Borohydride. *MSF* **2007**, *539-543*, 2295–2300. DOI: [10.4028/www.scientific.net/MSF.539-543.2295](https://doi.org/10.4028/www.scientific.net/MSF.539-543.2295).
  25. Kojima, Y.; Kawai, Y.; Nakanishi, H.; Matsumo, S. Compressed Hydrogen Generation Using Chemical Hydride. *J. Power Sources* **2004**, *135*, 36–41. DOI: [10.1016/j.jpowsour.2004.03.079](https://doi.org/10.1016/j.jpowsour.2004.03.079).
  26. Boran, A.; Erkan, S.; Ozkar, S.; Eroglu, I. Kinetics of Hydrogen Generation from Hydrolysis of Sodium Borohydride on Pt/C Catalyst in a Flow Reactor. *Int. J. Energy Res.* **2013**, *37*, 443–448. DOI: [10.1002/er.3007](https://doi.org/10.1002/er.3007).
  27. Xu, D.; Lai, X.; Guo, W.; Zhang, X.; Wang, C.; Dai, P. Efficient Catalytic Properties of SO<sub>4</sub><sup>2-</sup>/MxOy (M = Cu, Co, Fe) Catalysts for Hydrogen Generation by Methanolysis of Sodium Borohydride. *Int. J. Hydrogen Energy* **2018**, *43*, 6594–6602. DOI: [10.1016/j.ijhydene.2018.02.074](https://doi.org/10.1016/j.ijhydene.2018.02.074).
  28. Zou, Y. C.; Nie, M.; Huang, Y. M.; Wang, J. Q.; Liu, H. L. Kinetics of NaBH<sub>4</sub> Hydrolysis on Carbon-Supported Ruthenium Catalysts. *Int. J. Hydrogen Energy* **2011**, *36*, 12343–12351. DOI: [10.1016/j.ijhydene.2011.06.138](https://doi.org/10.1016/j.ijhydene.2011.06.138).
  29. Amendola, S. C.; Sharp-Goldman, S. L.; Janjua, M. S.; Kelly, M. T.; Petillo, P. J.; Binder, M. An Ultrasafe Hydrogen Generator: Aqueous, Alkaline Borohydride Solutions and Ru Catalyst. *ACS Division Fuel Chem.* **1999**, *44*, 846–866.
  30. Liu, C. H.; Chen, B. H.; Hsueh, C. L.; Ku, J. R.; Tsau, F. Novel Fabrication of Solid-State NaBH<sub>4</sub>/Ru-Based Catalyst Composites for Hydrogen Evolution Using a High-Energy Ball-Milling Process. *J. Power Sources* **2010**, *195*, 3887–3892. DOI: [10.1016/j.jpowsour.2009.12.087](https://doi.org/10.1016/j.jpowsour.2009.12.087).
  31. Chowdhury, A. D.; Agnihotri, N.; De, A. Hydrolysis of Sodium Borohydride Using Ru–Co-PEDOT Nanocomposites as Catalyst. *Chem. Eng. J.* **2015**, *264*, 531–537. DOI: [10.1016/j.cej.2014.11.108](https://doi.org/10.1016/j.cej.2014.11.108).
  32. Demirci, S.; Sahiner, N. Superior Reusability of Metal Catalysts Prepared within Poly (Ethylene Imine) Microgels for H<sub>2</sub> Production from NaBH<sub>4</sub> Hydrolysis. *Fuel Process Technol.* **2014**, *127*, 88–96. DOI: [10.1016/j.fuproc.2014.06.013](https://doi.org/10.1016/j.fuproc.2014.06.013).
  33. Guella, G.; Patton, B.; Miotello, A. Kinetic Features of the Platinum Catalyzed Hydrolysis of Sodium Borohydride from <sup>11</sup>B NMR Measurements. *J. Phys. Chem. C* **2007**, *111*, 18744–18750. DOI: [10.1021/jp0759527](https://doi.org/10.1021/jp0759527).
  34. Pena-Alonso, R.; Sicurelli, A.; Callone, E.; Carturan, G.; Raj, R. A Picoscale Catalyst for Hydrogen Generation from NaBH<sub>4</sub> for Fuel Cells. *J. Power Sources* **2007**, *165*, 315–323. DOI: [10.1016/j.jpowsour.2006.12.043](https://doi.org/10.1016/j.jpowsour.2006.12.043).
  35. Amendola, S. C.; Sharp-Goldman, S. L.; Janjua, M. S.; Spencer, N. C.; Kelly, M. T.; Petillo, P. J. A Safe, Portable, Hydrogen Gas Generator Using Aqueous Borohydride Solution and Ru Catalyst. *Int. J. Hydrogen Energy* **2000**, *25*, 969–975. DOI: [10.1016/S0360-3199\(00\)00021-5](https://doi.org/10.1016/S0360-3199(00)00021-5).
  36. Nasrollahzadeh, M.; Sajjadi, M.; Shokouhimehr, M.; Varma, R. S. Recent Developments in Palladium (Nano) Catalysts Supported on Polymers for Selective and Sustainable Oxidation Processes. *Coord Chem Rev* **2019**, *397*, 54–75. DOI: [10.1016/j.ccr.2019.06.010](https://doi.org/10.1016/j.ccr.2019.06.010).
  37. Tuan, D. D.; Lin, K. Y. A. Ruthenium Supported on ZIF-67 as an Enhanced Catalyst for Hydrogen Generation from Hydrolysis of Sodium Borohydride. *Chem. Eng. J.* **2018**, *351*, 48–55. DOI: [10.1016/j.cej.2018.06.082](https://doi.org/10.1016/j.cej.2018.06.082).
  38. Huang, Y. H.; Su, C. C.; Wang, S. L.; Lu, M. C. Development of Al<sub>2</sub>O<sub>3</sub> Carrier-Ru Composite Catalyst for Hydrogen Generation from Alkaline NaBH<sub>4</sub> Hydrolysis. *Energy* **2012**, *46*, 242–247. DOI: [10.1016/j.energy.2012.08.027](https://doi.org/10.1016/j.energy.2012.08.027).
  39. Corma, A.; Garcia, H.; Liabres, I.; Xamena, F. X. Engineering Metal Organic Frameworks for Heterogeneous Catalysis. *Chem. Rev.* **2010**, *110*, 4606–4655. DOI: [10.1021/cr9003924](https://doi.org/10.1021/cr9003924).
  40. Chen, C. W.; Chen, C. Y.; Huang, Y. H. Method of Preparing Ru-Immobilized Polymer-Supported Catalyst for Hydrogen

- Generation from  $\text{NaBH}_4$  Solution. *Int. J. Hydrogen Energy* **2009**, *34*, 2164–2173. DOI: [10.1016/j.ijhydene.2008.12.077](https://doi.org/10.1016/j.ijhydene.2008.12.077).
41. Xu, X.; Xi, Z.; Chen, W.; Wang, D. Synthesis and Structural Characterization of Copper (II) Complexes of Pincer Ligands Derived from Benzimidazole. *J. Coord. Chem.* **2007**, *60*, 2297–2308. DOI: [10.1080/00958970701261352](https://doi.org/10.1080/00958970701261352).
42. Dayan, O.; Özdemir, N.; Yakuphanoglu, F.; Şerbetci, Z.; Bilici, A.; Çetinkaya, B.; Tercan, M. Synthesis and Photovoltaic Properties of New Ru (II) Complexes for Dye-Sensitized Solar Cells. *J. Mater. Sci: Mater. Electron.* **2018**, *29*, 11045–11058. DOI: [10.1007/s10854-018-9187-9](https://doi.org/10.1007/s10854-018-9187-9).
43. Xu, D.; Zhao, L.; Dai, P.; Ji, S. Hydrogen Generation from Methanolysis of Sodium Borohydride over  $\text{Co}/\text{Al}_2\text{O}_3$  Catalyst. *J. Nat. Gas Chem.* **2012**, *21*, 488–494. DOI: [10.1016/S1003-9953\(11\)60395-2](https://doi.org/10.1016/S1003-9953(11)60395-2).